

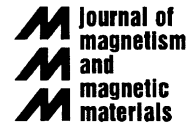


ELSEVIER

Available online at [www.sciencedirect.com](http://www.sciencedirect.com)

SCIENCE @ DIRECT®

Journal of Magnetism and Magnetic Materials 290–291 (2005) 227–230



[www.elsevier.com/locate/jmmm](http://www.elsevier.com/locate/jmmm)

# Highly coercive thin-film nanostructures

J. Zhou, R. Skomski\*, A. Kashyap<sup>1</sup>, K.D. Sorge, Y. Sui, M. Daniil, L. Gao,  
M.L. Yan, S.-H. Liou, R.D. Kirby, D.J. Sellmyer

*Department of Physics and Astronomy, Center for Materials Research and Analysis, University of Nebraska, Lincoln, NE 68588, USA*

Available online 2 December 2004

## Abstract

The processing, structure, and magnetism of highly coercive Sm–Co and FePt thin-film nanostructures are investigated. The structures include 1:5 based Sm–Co–Cu–Ti magnets, particulate FePt:C thin films, and FePt nanotubes. As in other systems, the coercivity depends on texture and imperfections, but there are some additional features. A specific coercivity mechanism in particulate media is a discrete pinning mode intermediate between Stoner–Wohlfarth rotation and ordinary domain-wall pinning. This mechanism yields a coercivity maximum for intermediate intergranular exchange and explains the occurrence of coercivities of 5 T in particulate Sm–Co–Cu–Ti magnets.

© 2004 Elsevier B.V. All rights reserved.

PACS: 75.50; 75.60; 75.75

Keywords: Coercivity; Hard magnetic materials; Magnetic nanostructures; Domain-wall pinning; Magnetization reversal

## 1. Introduction

Hard-magnetic thin films are of interest for present or future applications such as magnetic microelectromechanical systems, microstructured magnetic sensors, spin electronics, and magnetic data storage. Beyond the pronounced magnetocrystalline anisotropy of underlying compounds such as SmCo<sub>5</sub> [1] and FePt [2], the development of coercivity is facilitated by thin-film specific nanostructuring [3] and, to some degree, by exploiting surface and interface anisotropies [4]. Examples of coercive thin-film nanostructures are thin [5] and ultrathin [6,7] L<sub>10</sub> structures

(mostly FePt), granular Sm–Co-based thin films [8], and Fe/W(1 1 0) [4].

As in bulk materials, details of the nano- or microstructure have a pronounced effect on the coercivity. For non-interacting perfect small spheres one expects the coercivity to approach the Stoner–Wohlfarth prediction, but this is an idealized and difficult-to-realize limit, since grain imperfections and intergranular interactions interfere [3,9]. However, many open questions remain concerning the transition from localized reversal or curling to Stoner–Wohlfarth-like coherent rotation. Furthermore, some materials, such as magnetic nanotubes [10], need separate consideration.

In this paper, we study some nanostructural aspects of highly coercive magnetic thin films. The following systems are being analyzed: Sm–Co–Cu–Ti particulates; FePt:C nanocomposites film; FePt nanotubes formed by hydrogen reduction; and FePt L<sub>10</sub> nanostructures prepared by focused ion-beam (FIB) milling.

\*Corresponding author. Tel.: +1 402 472 2682; fax: +1 402 472 2879.

E-mail address: [rskomski@unlserve.unl.edu](mailto:rskomski@unlserve.unl.edu) (R. Skomski).

<sup>1</sup>Present address: IFW Dresden, D-01171, Dresden, Germany

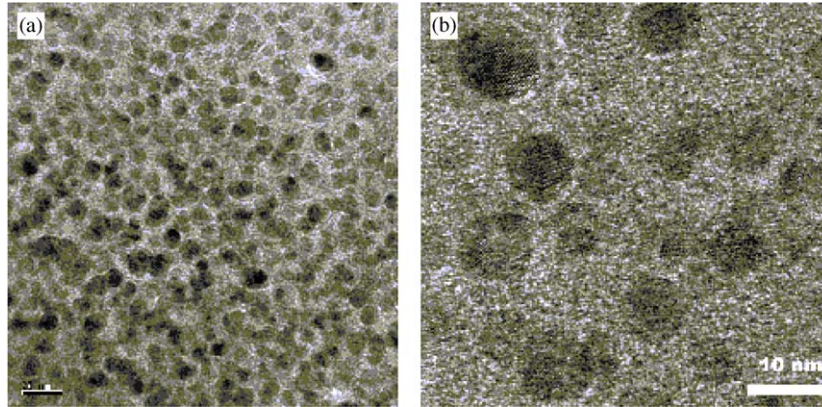


Fig. 1. Structure of a particulate Sm–Co–Cu–Ti thin film: (a) TEM and (b) HRTEM. The scale bars in (a) and (b) are 20 and 10 nm, respectively.

## 2. Experimental systems

### 2.1. Sm–Co-based particulate thin films

Sm–Co–Cu–Ti particulate thin films were prepared by magnetron sputtering. Sm–Co/CuTi multilayered films, sandwiched between Cr layers, were sputtered on Si(1 0 0). A typical film contains 38 units of 45 Å SmCo<sub>5</sub> and 7 Å CuTi, and proper heat treatment yields spheres of 8 nm diameter embedded in a matrix [8]. Transmission electron microscopy (TEM) shows that the phases have a composition close to SmCo<sub>5</sub>, and the matrix is likely Cu-rich. The room temperature coercivity of the granular film is 5.04 T. Fig. 1 shows TEM (a) and high-resolution TEM (b) micrographs of the annealed sample.

### 2.2. L1<sub>0</sub>-based thin films

The FePt-based magnetic thin films were prepared by sputtering multilayers with the structure [C(3 Å)/Fe(9 Å)/Pt(10 Å)]<sub>5</sub>/C(50 Å), followed by rapid annealing for about 10 min. The films exhibit perpendicular anisotropy and a coercivity of 0.85 T. Fig. 2 shows that L1<sub>0</sub>-phase FePt nanograins with sizes of about 10 nm are embedded in a C matrix [5].

Nanostructures with perpendicular anisotropy and arbitrary geometries down to feature sizes of less than 50 nm may be created by FIB milling of FePt thin films with perpendicular anisotropy. However, preliminary experiments on sub-micrometer nanorings [11] indicate a deterioration of the structure and a corresponding coercivity reduction.

A recently developed method for creating highly coercive magnetic nanotubes is hydrogen reduction in nanochannels of porous alumina templates [10]. Loading the templates with a mixture of Fe and Pt chlorides,

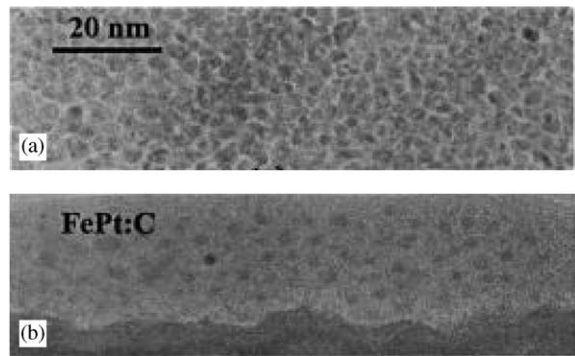


Fig. 2. TEM of a FePt:C film: (a) bright-field image and (b) cross-section image [5].

followed by hydrogen reduction at 560 °C, yields ferromagnetic FePt nanotubes in the alumina pores. The length of the nanotubes is about 50 μm and their diameters range from about 150 to 220 nm, depending on the thickness of the template film and the pore diameter distribution. A typical coercivity is 2.1 T.

## 3. Coherent rotation and discrete pinning

To understand the magnetization reversal in granular systems, it is necessary to consider the role of intergranular exchange and magnetostatic interactions. In the absence of interactions, the magnetization reversal in small magnetic particles is Stoner–Wohlfarth like, although the coercivity tends to be smaller than the Stoner–Wohlfarth prediction.

There are two length scales involved, both unrelated to the critical single-domain size [3]. First, when the particles are smaller than about 20 nm, coherent rotation is more favorable than magnetization curling.

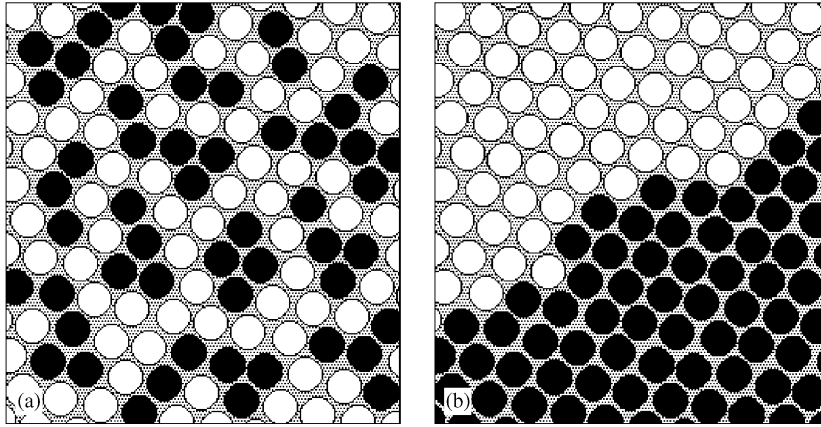


Fig. 3. Reversal mechanisms in granular magnets: (a) Stoner–Wohlfarth rotation and (b) discrete pinning. The black-and-white contrast indicates opposite magnetization directions.

Second, nucleation sites comparable to or larger than the domain wall width (about 5 nm) yield localized nucleation and a strong coercivity reduction.

Intergranular exchange, and magnetostatic interactions, modify the coercivity of granular magnets. Atomically, it matters whether the matrix is ferromagnetic, paramagnetic, or insulating [3,12,13], but for small and weakly coupled grains, the exchange can be modeled by a single parameter  $J$ . (In general, the calculation of  $J$  involves an integration over all exchange paths and differs from what one would expect by counting the surface atoms of adjacent grains.)

Analyzing the dependence of the reversal mechanism as a function of increasing  $J$  yields a transition from Stoner–Wohlfarth behavior to a discrete pinning regime. In both cases, magnetization reversal is realized by the switching of individual grains, as compared to an essentially continuous domain wall motion. But in the discrete pinning regime there are correlations reminiscent of interaction domains. Fig. 3 illustrates the difference by showing schematic magnetization configurations close to coercivity.

A characteristic feature is a coercivity maximum at the transition between nucleation and discrete domain-wall pinning. Small exchange hardens grains that are soft due to imperfections or local stray fields, whereas strong exchange facilitates domain-wall motion.

In a numerical analysis [14], the material of Section 2.1 was modeled as  $\text{SmCo}_5$  particles with an average size of 8 nm on a rectangular lattice. We considered three layers, each having 9  $\text{SmCo}_5$  spheres. The particles are randomly oriented and embedded in a matrix with different magnetic properties ( $\mu_0 M_s = 0.88 \text{ T}$ ,  $A = 25 \text{ pJ/m}$ , and  $K_1 = 2 \times 10^6 \text{ J/m}^3$ ). Fig. 4 shows the calculated hysteresis for the discrete-pinning regime. The coercivity of the model film is 5.5 T, close to the experimental value.

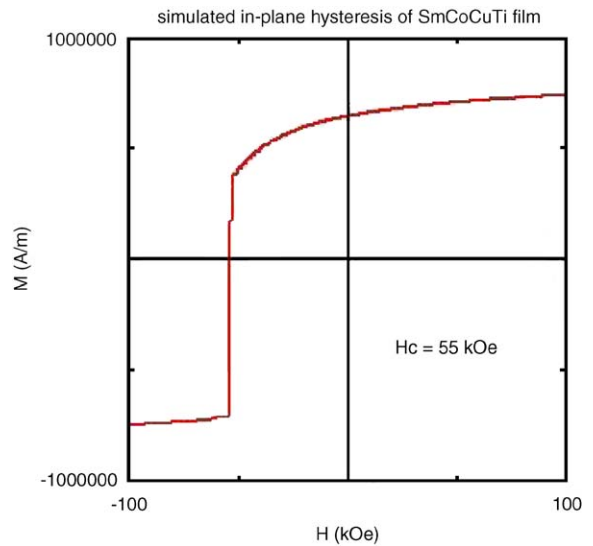


Fig. 4. Simulated hysteresis curve of a Sm–Co–Cu–Ti film.

#### 4. Discussion and conclusions

The above discrete-pinning mechanism is limited to granular magnets. Whereas other mechanisms are realized in structures such as nanotubes and nanorings. For example, in spheres and cylinders, the curling mode contains a line at  $\mathbf{r} = z\mathbf{e}_z$  where  $\mathbf{M}(\mathbf{r}) = M_s \mathbf{e}_z$  by symmetry [10]. Magnetic nanotubes and nanorings do not suffer from this restriction, so that the transition from curling to coherent rotation happens at a much smaller transition radius, depending on the ratio between inner and outer radius.

Most structures considered in this paper are very hard, with coercivities much larger than 1 T. However, thin-film nanostructuring is also a useful tool to create

semi-hard structures. For example, hydrogen processing also has been used to produce  $\text{Fe}_3\text{O}_4$  nanotubes having a coercivity of 0.061 T. Another example is nanodot structures for magnetic information processing, where the switching behavior of magnetic nanodots could be used to realize logic gates [15,16].

In conclusion, thin-film specific fabrication techniques, such as magnetron sputtering and hydrogen processing, make it possible to produce magnetic nanostructures with high and often well-controlled coercivities. In addition, the structures offer insight into the physics of magnetization reversal, as exemplified by the discrete pinning mechanisms and tubular curling modes.

This research is supported by DOE, AFOSR, NSF-MRSEC, the W.M. Keck Foundation, and CMRA.

## References

- [1] K. Kumar, *J. Appl. Phys.* 63 (1988) R13.
- [2] R.A. McCurrie, *Ferromagnetic Materials—Structure and Properties*, Academic, London, 1994.
- [3] D. Sander, R. Skomski, C. Schmidhals, A. Enders, J. Kirschner, *Phys. Rev. Lett.* 77 (1996) 2566.
- [4] R. Skomski, *J. Phys. CM* 15 (2003) R841.
- [5] M.L. Yan, X.Z. Li, L. Gao, S.H. Liou, D.J. Sellmyer, R.J.M. van de Veerdonk, K.W. Wierman, *Appl. Phys. Lett.* 83 (2003) 3332.
- [6] K. Kang, Z.G. Zhang, C. Papusoi, T. Suzuki, *Appl. Phys. Lett.* 84 (2004) 404.
- [7] M. Weisheit, L. Shultz, S. Fähler, *J. Appl. Phys.* 95 (2004) 7489.
- [8] J. Zhou, A. Kashyap, Y. Liu, R. Skomski, D.J. Sellmyer, *IEEE. Trans. Magn.* 40 (2004) 2940.
- [9] A. Aharoni, *Introduction to the Theory of Ferromagnetism*, Oxford University Press, Oxford, 1996.
- [10] Y.C. Sui, R. Skomski, K.D. Sorge, D.J. Sellmyer, *Appl. Phys. Lett.* 84 (2004) 1525.
- [11] K.D. Sorge et al., *Scripta Materialia* (2005), in press.
- [12] R. Skomski, D. Leslie-Pelecky, R.D. Kirby, A. Kashyap, D.J. Sellmyer, *Scripta Mater.* 48 (2003) 857.
- [13] R. Skomski, A. Kashyap, Y. Qiang, D.J. Sellmyer, *J. Appl. Phys.* 93 (2003) 6477.
- [14] Using the OOMMF NIST code, the Landau–Lifshitz–Gilbert equation is solved for various magnetic field values. Details will be published elsewhere.
- [15] K.D. Sorge, A. Kashyap, R. Skomski, L. Yue, L. Gao, R.D. Kirby, S.H. Liou, D.J. Sellmyer, *J. Appl. Phys.* 95 (2004) 7414  
K. D. Sorge, et al., 2003 APS March Meeting, Austin, TX V28.4.
- [16] S. Anisul Haque, M. Yamamoto, R. Nakatani, Y. Endo, *Sci. Techn. Adv. Mater.* 5 (2004) 79.